Evaluation of reductants used for ilmenite smelting based on CO_2 reactivity (Boudouard reaction) measurement

by P. Jordan*

Synopsis

The practice of ilmenite smelting in electric arc furnaces has been researched and published over the last few decades. An issue that has not been addressed is the understanding of the properties of ilmenite smelting reductants, and linking these properties to the subsequent smelting behaviour in the furnace. The reduction mechanism of ilmenite smelting is not fully understood, but it is believed that the Boudouard reaction plays a role. This paper investigates the behaviour of a number of reductants when reacted with CO_2 at different temperatures.

Keywords

Boudouard reaction, carbon reactivity, reductants, ilmenite smelting.

Introduction

Ilmenite has a nominal composition of $FeO.TiO_2$. South African ilmenite is close to this nominal composition, with the main impurities being MnO, MgO, SiO_2 and Al_2O_3 which contribute to about 3% of the mass of the ilmenite.

TiO_2 is an excellent opacifier and used as a white pigment in paint, paper and plastics. The first step in upgrading the ilmenite to a pure TiO_2 product is smelting the ilmenite to produce a TiO_2 rich slag of 80-90% TiO_2 content. During ilmenite smelting, the iron content of the oxide is lowered by reduction to metallic iron, which takes place in the liquid state at temperatures around 1650°C. This process produces two products, a titania-rich slag and molten iron, the only by-product being the off-gas. Ilmenite smelting is conducted in electric open arc furnaces (AC or DC) to provide the required energy input.

The slag is then processed further. There are two main routes, the chloride and the sulphate route, that are used in the upgrading of the slag to serve as feedstock for the production of the TiO_2 pigment.[1] Increasingly, TiO_2 pigment is produced via the chloride route. This route involves the chlorination of the feed stock in a fluidized bed to yield volatile chlorides, which are separated to give pure $TiCl_4$ which is then oxidized to form pure TiO_2.

There are only two feed materials, ilmenite and the reductant. One of the constraints limiting the operating range of ilmenite smelters is the slag composition. The reason for this is that the chlorination process can manage only low levels of impurities, mainly because of the effect of impurities such as MgO and CaO on the stability of the fluidized bed chlorinator. Table I shows the typical specification of the slag used in the chloride process.[2] This strict specification on impurities implies that no fluxing addition can be made, and more importantly, that the impurities in the reductant need to be limited, hence severely limiting the number of reductants that can be used.

A schematic representation of the process mechanism is shown in Figure 1. The mechanism proposes thermo-chemical equilibrium and transient cooling and solidification of the liquid slag at the interface between the slag and metal baths, followed by a re-melting of the solidified slag.[3] This provides a mechanism to describe M_3O_5 formation in the slag. However, other mechanistic steps remain unclear. These include carbon transfer to the metal, which must account for the fact that the carbon content far exceeds the amount for the slag-metal equilibrium, and the reduction reaction itself. This reduction mechanism is presumed to be sustained by a gas halo, containing largely CO gas and some CO_2, which surrounds

* Exxaro Resources, Pretoria, South Africa.

Evaluation of reductants used for ilmenite smelting based on CO_2 reactivity
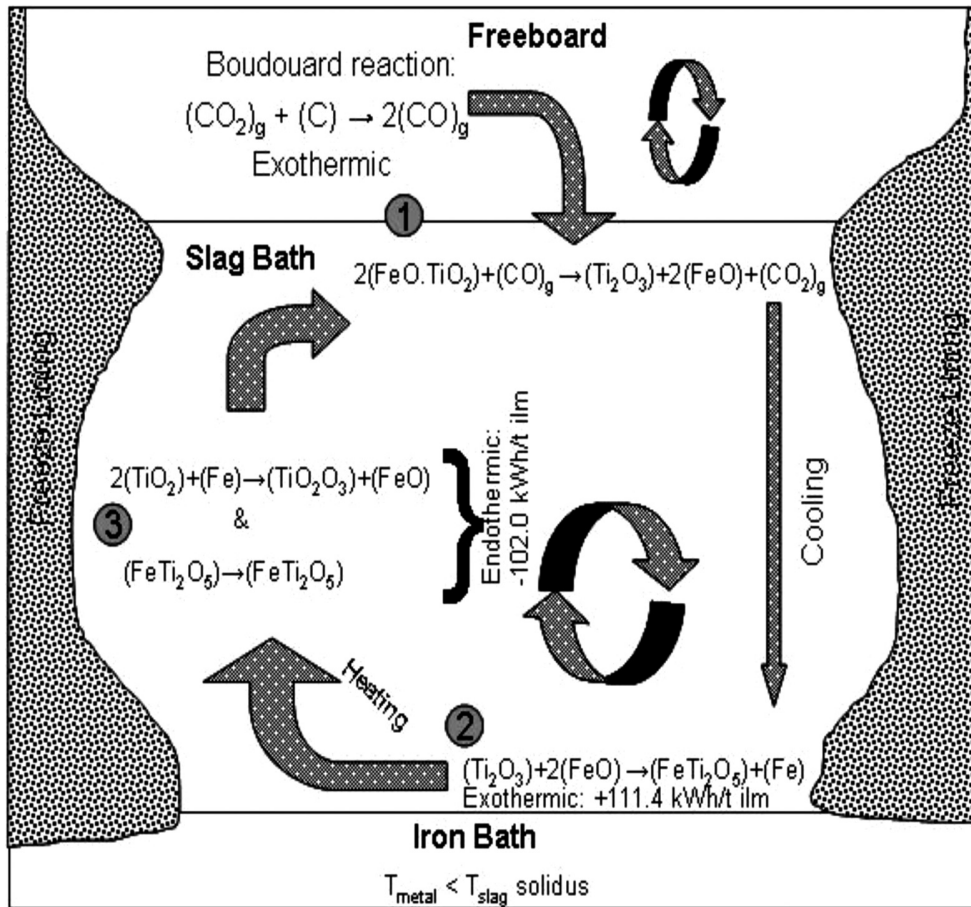
Figure 1—Smelting mechanism for ilmenite in a DC arc furnace, schematic derived from Pistorius[3]

Table I	
Typical specification of slag[2]	
Typical Specification of slag used in the chloride process (mass %)	
Total % TiO_2	>85.0
% Ti_2O_3	<35.0
% FeO	<12.0
% SiO_2	<2.0
% Al_2O_3	<1.5
% CaO	<0.13
% MgO	<1.2
% MnO	<2.0
% Cr_2O_3	<0.25
% V_2O_5	<0.60

the reductant particles.[4] Due to the lower density of the reductant particles they are expected to float on top of the slag bath until fully reacted. The proposed reaction mechanism then involves the following:

➤ Reduction of FeO and TiO_2:

$$FeO + CO \rightarrow Fe + CO_2 \qquad [1]$$

$$2TiO_2 + CO \rightarrow Ti_2O_3 + CO_2 \qquad [2]$$
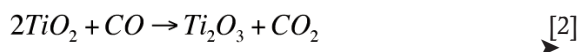
➤ Mass transfer of CO_2 through the gas halo to the reductant.

➤ Regeneration of the CO gas through the Boudouard reaction:

$$CO_2 + C \rightarrow 2CO \qquad [3]$$

Due to the reductant and slag being separated by a gas halo, the formation of TiC is not expected as the reaction $3Ti_2O_3 + CO \rightarrow TiC + 5TiO_2$ has a equilibrium constant of $K = 1.6 \times 10^{-4}$ at 1650°C and is thus unlikely to form TiC.

At the high operating temperatures of the smelter, the rate of the Boudouard reaction is not expected to be rate limiting, the regeneration of CO is assumed to be efficient,

Evaluation of reductants used for ilmenite smelting based on CO_2 reactivity
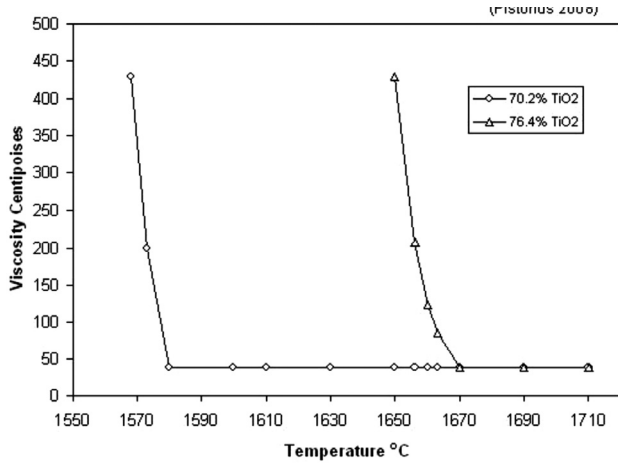
Figure 2—Change in viscosity of QIT slags with temperature; the sharp increase in viscosity at lower temperatures is the result of partial solidification[5]

and the gas in the halo to be nearly pure CO. However, the rate of the Boudouard reaction could have a significant impact on the furnace behavior and stability of the smelting process. One such impact is on the phenomenon known as slag foaming, which is both dangerous and disruptive to stable operation. It has been proposed that second phase particles (reductant) act as gas nucleation sites. This, combined with the reactivity of the reductant, the Boudouard reaction being endothermic, and the steep change in viscosity with minimal temperature change of the slag, as shown in Figure 2, are responsible for foaming in the furnace.

This foaming can lead to process instabilities such as loss of arc, bank formation in the upper parts of the furnace freeboard, and more severely-blockages in the off-gas ducts.

Differences in the reaction rate of reductants could account for the different behaviors observed in the smelting furnace. Understanding the reaction kinetics and the influence it exerts on the smelting behaviour could help in the optimal selection of a reductant and assertaining whether reductants could be blended to optimize process stability.

To measure the Boudouard reaction kinetics of carbon reductants on a laboratory scale, the data is essentially recorded as a mass loss over time. The mass loss or in other words the mass of carbon converted to gas (Equation [3]) is then expressed as a ratio of the lost mass to the initial mass or remaining mass. In utilizing the off-gas measurements, the CO content is measured in conjunction with the gas flow rate, and this is then used to calculate the mass of carbon converted to CO. This method doe, however, have some pitfalls. The ideal is to obtain equipment where results are measurement instantaneous and hence not obscuring the time measurement. Thus, utilizing the measurement of mass seems to be the preferred method.

There are numerous ways of expressing the kinetics of Boudouard or steam gasification reactions, with the most common of these being the shrinking core model and the homogeneous model. The aim of kinetic modelling is to use simple equations to predict the reaction process. The shrinking core and homogeneous models are the simplest, and are based on the assumption that the reaction rates are chemically controlled[6].

The shrinking core model assumes that the reaction occurs at an external surface of the char particle and gradually moves inwards, leaving an porous ash layer behind. At intermediate conversion of the solid reactant, there is a shrinking core of the unreacted solid, which diminishes as the reaction proceeds. The shrinking core model[6] is described mathematically as:

$$\frac{dx}{dt} = \kappa\left(1-x\right)^{2/3} \, or \, 1-\left(1-x\right)^{1/3} = \kappa t \qquad [4]$$

where x is the fractional conversion of carbon reacted over initial carbon on a dry ash free basis at a specific time.

Comparing the reactivities of different reductants is usually quantified by the reactivity index R [6] that is defined as:

$$R = \frac{0.5}{\tau_{0.5}} \qquad [5]$$

where R is the reactivity index, 0.5 is the fractional conversion and $\tau_{0.5}$ the time required to reach 50% conversion of the carbon. The R values can be calculated from the conversion (x) versus time (t) relationship.

The apparent reaction rate [7] method gives an instantaneous reaction rate at any level of conversion. This method is used to study whether or not the reaction rate increases or decreases over time as a function of the concentration of the ash or slag on the active sites of the reductant particle. It is believed that some oxide species could act as catalysts, enhancing the reaction rates, while the composition of the oxide species could potentially result in a slag that could coat the particle and retard the reaction rate. The apparent reaction rate is expressed as grams of reacted carbon per grams of remaining carbon per second, this is described as:

$$R_{app} = \frac{1}{w}\left(\frac{dw}{dt}\right) \, \left[g.g^{-1} \cdot s^{-1}\right] \qquad [6]$$

where R_{app} is the apparent reaction rate in gram per gram per second ($g.g^{-1}.s^{-1}$) and w is the weight of carbon remaining at time t.

Parameters exerting an influence on the Boudouard reaction rates could be grouped in three major groups:

➤ Environment, (temperature, gas composition and flow rates, and pressure)
➤ Physical characteristics, (size, shape, pores and density) and
➤ Chemical characteristics, (elemental composition, petrography, degree of graphitization).

The environment is controlled by the test or experimental procedure. Physical characteristics such as particle size and shape could be controlled to a certain extent. The chemical characteristics are in most part a function of the coal geology, deposition, and depositional environment of the original coal deposit, and here no or very little control could be exerted on

Evaluation of reductants used for ilmenite smelting based on CO$_2$ reactivity

the sample. Thus the chemical characteristics and some physical characteristic are related essentially to the differences in reaction kinetics, in order to explain the reaction kinetics and the impact of these characteristics on the utilized process technology.

Methods and materials

Four different anthracites that are commercially used in the ilmenite smelting industry were selected for the test work. Table II gives the proximate and ultimate analysis, Table III

the ash compositions of the samples, and Table IV the petrographic results.

The CO$_2$ reactivity tests were carried out in a tube furnace (tube dimensions: approximately 7.5 cmØ and 90 cm length) heated to the desired temperature (1100°C and 1600°C) while purging with argon gas at a rate of 200 sccm (standard cubic centimeters per minute). The gas was introduced at the top of the tube. In the process of heating, the crucible was placed at the bottom tip of the tube to minimize thermal shock on both the crucible and the tube when inserting the sample. After

Table II

Proximate and ultimate analysis of anthracites

	S_1	S_2	S_3	S_4
% Moisture (air-dried)	2.8	1.0	3.6	2.8
% Ash (dry basis)	8.7	6.2	3.7	8.7
% Volatile matter (dry basis)	4.9	5.6	1.7	4.9
% Fixed carbon (air-dried)	84.0	87.4	91.2	84.0
% Carbon (dry basis)	85.2	88.2	92.8	85.2
% Hydrogen (dry basis)	2.40	3.06	1.30	2.40
% Oxygen (dry basis)	0.99	0.76	0.56	0.99
% Nitrogen (dry basis)	1.79	1.20	0.87	1.79
% Sulphur (dry basis)	0.88	0.59	0.82	0.88

Table III

Ash constituent analysis of anthracites (wt%, on ash)

	S_1	S_2	S_3	S_4
%Al$_2$O$_3$	29.95	30.49	20.74	26.51
%CaO	1.55	1.31	6.58	0.66
%Cr$_2$O$_3$	0.11	0.07	1.06	0.06
%Fe$_2$O$_3$	13.74	7.80	19.89	12.46
%K$_2$O	3.49	3.45	2.30	3.67
%MgO	1.02	1.04	4.36	0.93
%MnO	0.15	0.06	0.21	0.15
%Na$_2$O	0.51	0.45	1.23	0.17
%P$_2$O$_5$	0.22	0.32	0.15	0.14
%SiO$_2$	46.56	53.56	34.71	53.30
%TiO$_2$	1.97	0.95	1.60	1.64
%V$_2$O$_5$	0.06	0.06	0.13	0.05
%ZrO$_2$	0.12	0.13	0.06	0.08
%Ba	0.06	0.10	0.40	0.05
%Sr	0.07	0.03	0.25	0.01
%SO$_3$	1.01	0.67	6.72	0.55

Table IV

Petrographic analysis of anthracites

	S_1	S_2	S_3	S_4
% Vitrinite	48	94	81	84
% Fusinite	24	2	8	7
% Macrinite	21	1	4	3
% Total inertinite	45	3	12	10
% Heat altered	2	0	1	0
% Graphitized vitrinite	1	0	1	1
% Visible mineral matter	4	3	2	5
Rank % reflectance	3.35	2.88	5.34	5.45

Evaluation of reductants used for ilmenite smelting based on CO$_2$ reactivity

reaching the test temperature, the sample (-8 +5.6 mm) was charged into the crucible and lifted to the hot zone (about 38 cm from the bottom end of the tube) and argon gas was substituted by carbon dioxide (CO$_2$) at a flow rate of 150 sccm. The initial mass was logged and thereafter the mass was logged in 30 second intervals.

For the 1100°C experiments, the tests were performed over a period of 6 hours, and for the 1600°C experiments over 24 hours. Thermogravimetric curves of all the tests were drawn depicting the percentage mass loss over time.

An apparent reaction rate was calculated for every 900 second interval after ignoring the initial period connected to volatile matter loss. The apparent reaction rate was calculated utilizing Equation [6].

Results and discussion

The carbon conversion x is defined as the ratio of the gasified carbon to the initial carbon in the anthracite char (on a dry ash-free basis) as given in Equation [7]:

$$x(t) = \frac{C_0 - C_t}{C_0} \qquad [7]$$

where C$_0$ represents the initial carbon weight and $C_{(t)}$ represents the carbon weight at reaction time t. Figures 3 and 4 illustrate the relationship of x with t for the four samples at 1100°C and 1600°C respectively.

It is interesting to note the different order observed for sample S_2 and S_4, for the 1100°C to 1600°C experiments respectively, and this could be seen as the influence of the ash composition with respect to its melting behaviour, i.e. slag formation, as the carbon is depleted and the mineral matter concentrated and melted.

From this data, the conversion factor x can be determined and used in the shrinking core model as per Equation [4], plotting 1-(1-x)$^{1/3}$ over time to obtain K. Figures 5 and 6 show the linear plots for 1100°C and 1600°C, respectively.
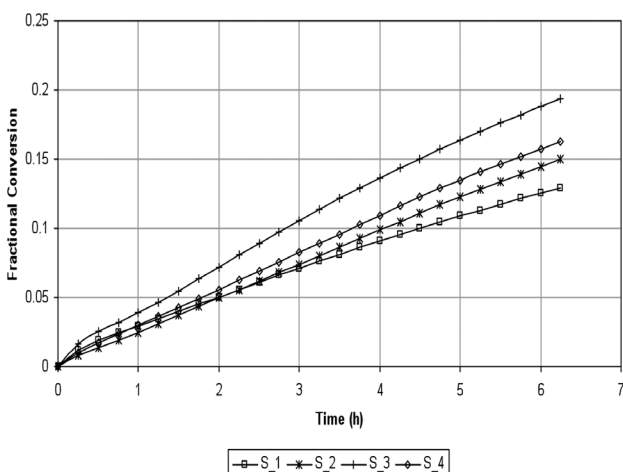
The homogenous model -ln(1-x) vs time was also investigated, but it was found that it could describe only the lower reactive anthracites at 1100°C (S_1 and S_4) to a certain degree of accuracy.

It was thus concluded that the shrinking core model describes the CO$_2$ gasification of the anthracite samples best at lower and higher temperatures. Many investigators, as cited by Zang *et al*.[6], have also reported good agreement
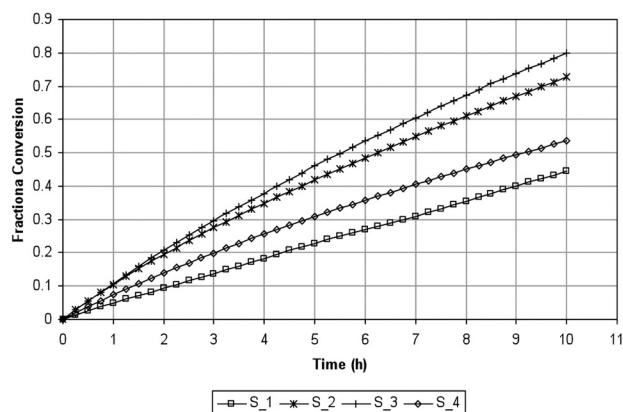

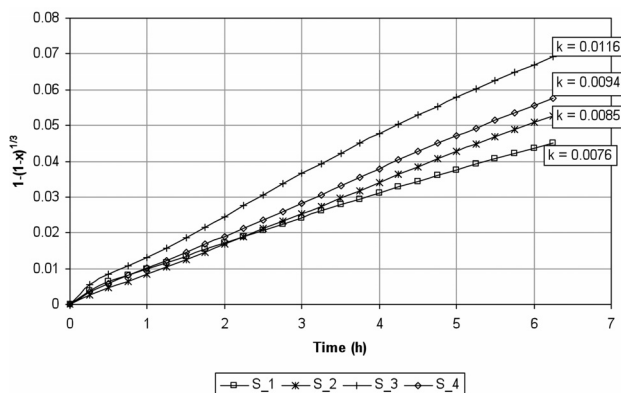Figure 4—Fractional conversion of the anthracite samples at 1600°C

Figure 5—Shrinking core model plot of 1-(1-x)1/3 against time for the anthracite chars produced at 1100°C

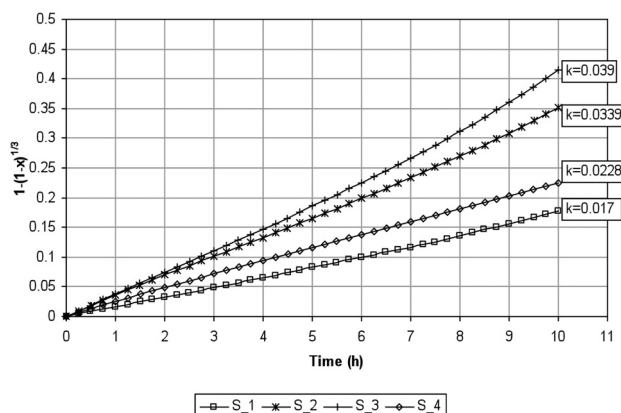Figure 3—Fractional conversion of the anthracite samples at 1100°C

Figure 6_Shrinking core model plot of 1-(1-x)1/3 against time for the anthracite chars produced at 1600°C

Evaluation of reductants used for ilmenite smelting based on CO_2 reactivity

between the predictions of this model and their experimental data, and also obtained the same conclusion with regard to the homogenous model.

Equation [5] is widely used to differentiate between different reductants based on their CO_2 reactivity, including reactivities above a 50% conversion rate. Utilizing this equation, Figures 7 and 8 are obtained, which show the Reactivity Index for both the 1100°C and 1600°C heated samples for conversions of 20% to 60% for the 1100°C heated sample and 20% to 70% for the 1600°C sample.

It is interesting to note that in Figure 7 the samples S_4 and S_3 give identical reactivity indices, but at 1600°C the reactivity indices are clearly different. This confirms the decision to investigate reductant reactivity at temperatures close to the temperatures that would be experienced by the reductant in the process. Another point to note is the almost constant reactivity index of the low reactive samples compared to the decrease in reactivity of the higher reactive samples, and this is also more profound at higher temperatures. This could be explained by the ash layer formation around the particle. At higher temperatures the liquidus temperature, of the ash is exceeded and a liquid layer is formed as compared to a dry, brittle ash layer at lower temperatures.

To calculate the apparent reaction rate[7] of the reductant at conversion levels, Equation [6] is utilized. Figures 9 and 10 show the apparent reaction rate of the anthracite chars at different fractional conversions for the temperatures at 1100°C and 1600°C respectively.

From the apparent reaction rate data plots in Figure 9 it appears that there is little or no influence of the ash layer for sample S_2 and S_4. For sample S_3, it appears to be catalytically increased up to a level of 8% conversion and then retarded. The apparent reaction rate of sample S_1 seems to decrease constantly as the conversion proceeds.

At an elevated temperature, the apparent reaction rate differs significantly, as shown in Figure 10. Here sample S_4 still seems to have a constant apparent reaction rate, and sample S_1 reaches almost identical reaction rates as sample S_4 from a conversion of 33%. Samples S_2 and S_3, however, seem to be greatly affected as the carbon conversion increased.

Temperature has not only a profound effect on the rate at which the Boudouard reaction occurs, but has a greater effect on the influence of the mineral constituents within the reductant and how they interact with each other, the carbon and the carbon dioxide environment to form an ash/slag layer around the reductant particle. The temperature regime and the mineral compositions govern the amount of phases and subsequent viscosity of these phases to be formed, which could lead to different effects on the reaction rate at different temperature regimes.

On examining the relation between the petrographic analysis, rank, and maceral composition of the parental anthracites and their resulting reactivity, no direct correlation could be found to explain the different reaction rates.

However, it should be stated that the resulting anthracite chars were not characterized in this work, and would form part of the ongoing investigation to explain the different behaviours of the reductants.

To investigate the ash/slag formation by the different reductants, a FactSage™ model was developed to simulate the isothermal equilibrium composition of the different ash components, with the assumption that the process reaches
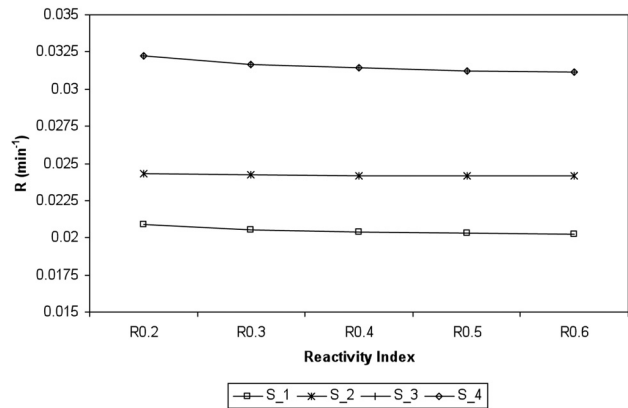

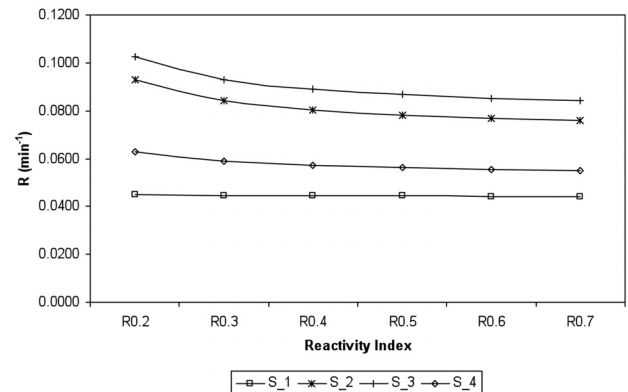Figure 7—Reactivity index of the anthracite samples at different levels of conversion at 1100°C

Figure 8—Reactivity index of the anthracite samples at different levels of conversion at 1600°C
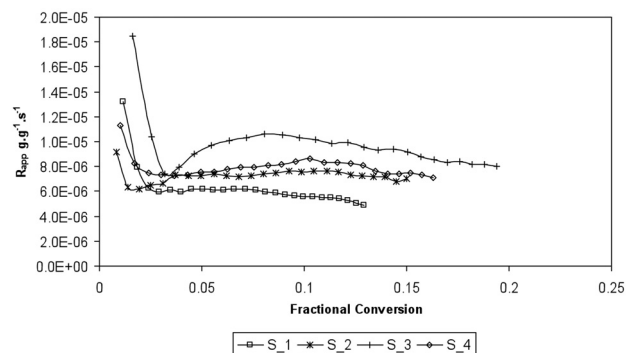

Figure 9—Apparent reaction rate of anthracite chars vs. fractional conversion at 1100°C

Evaluation of reductants used for ilmenite smelting based on CO_2 reactivity
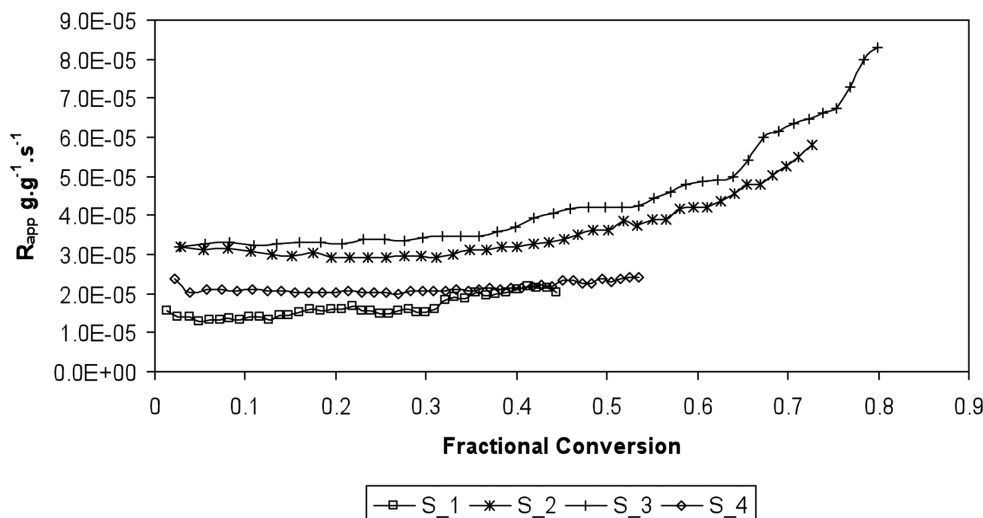
Figure 10—Apparent reaction rate of anthracite chars vs. fractional conversion at 1600°C

Table V

Resulting isothermal percentage mass equilibrium composition at 1100°C and 1600°C for a system where no carbon was added

	S_1		S_2		S_3		S_4	
	1100°C	1600°C	1100°C	1600°C	1100°C	1600°C	1100°C	1600°C
%Gas	1.99	5.99	1.20	4.53	7.65	11.38	1.45	5.02
%Slag	57.04	93.88	63.93	95.34	28.41	87.97	64.50	94.92
% Spinel	35.70	0	31.16	0	14.25	0	33.25	0
%Pyroxene	3.93	0	3.21	0	47.61	0	0.01	0
%Metal	0.13	0.13	0.13	0.13	0.65	0.65	0.06	0.06
%Other solids	1.22	0	0.38	0	1.42	0	0.72	0

Table VI

Resulting isothermal percentage mass equilibrium composition at 1100°C and 1600°C for a system with excess carbon

	S_1		S_2		S_3		S_4	
	1100°C	1600°C	1100°C	1600°C	1100°C	1600°C	1100°C	1600°C
%Gas	55.15	73.00	59.80	76.63	57.22	72.57	59.75	75.24
%Slag	3.06	0	2.72	0	5.21	0	0.81	0
% Spinel	0	0	0	0	0	0	0	0
%Pyroxene	0	0	0	0	0	0	0	0
%Metal	18.80	27.00	13.74	23.37	22.45	27.43	18.04	24.76
%Other solids	22.98	0	23.75	0	15.12	0	21.41	0

equilibrium within the reaction time. The ash composition (as shown in Table III, dry volatile matter free basis) was used as input to the FactSage model. This ash was then equilibrated without any carbon and with an excess amount of carbon at 1100°C and 1600°C. From the FactSage modelling the mass percentage of the resulting phases was determined for a system where no carbon was added (shown in Table V) and where an excess of carbon was added (Table VI).

The modelling results for when no carbon is added shows that slag is the major phase that forms (comprising mainly SiO_2, Al_2O_3, K_2O, CaO, MgO and MnO). As expected, with an increase in temperature the amount of slag also increases significantly. As discussed earlier this can inhibit the Boudouard reaction. At 1100°C some spinel and pyroxene phases are also present, which can potentially act as catalysts.

Evaluation of reductants used for ilmenite smelting based on CO_2 reactivity

For the scenario where an excess of carbon is present, the products that form are significantly different. Firstly, a large amount of gas is formed, consisting mostly of CO due to reduction of the various oxides. In addition, the gas contains a large amount of SiO and lesser amounts of alkalis. This certainly is the case for ilmenite smelting, where it has been reported[8] that the furnace dust obtained is significantly enriched in Si, Mn and K. Furthermore, it is also relevant to note the large amount of metal that is produced. At 1100°C the metal consists mainly of Fe and Si, while at the higher temperature large amounts of Al are also present in addition to the Fe and Si, due to the strongly reducing conditions. It is interesting to note that at these strongly reducing conditions FactSage predicts very little slag, as all the oxides are reduced to the metal phase or report to the gas phase.

The scenarios in Table V and VI set out the two extremes which can be expected if the systems reached equilibrium. In reality it is expected that the end result should be between the two extremes. It is highly unlikely all the minerals in the reductant would be reduced to metal as is shown in Table VI, and some pyroxenes and spinels could still be present, especially at the lower temperature. This is one of the aspects that requires further investigation, as this could give insight into the catalytic and coating effect of the slags and the way in which they affect the CO_2 reactivity.

Conclusion

From the study of the four anthracites commercially used by ilmenite smelters, it was found that the rate of the Boudouard reaction could be used as a behavioral analysis to distinguish between the different reductants used in the ilmenite industry. By analysing the reaction rates at elevated temperatures, closer to those of the actual process, results in different rankings of the anthracites. On discussing these results with the furnace operating staff, it would appear that the furnace stability experienced does relate to the CO_2 reaction rate of the reductants. More reactive reductants tend to result in greater furnace stability than the lower reactive reductants. This will need to be quantified in further studies.

The role of anthracite kinetics in CO_2 gasification is well described by the shrinking core model. However, using the reactivity index method could lead to different anthracites appearing to behave similarly. By applying the apparent reaction rate as per Equation [5] the instantaneous reaction rates showed the behaviour of the reductant over time.

The rank and maceral composition of the parent anthracites did not appear to be related to the reactivity of these anthracites at 1100°C or 1600°C. Although the influence of the carbon structure, i.e. level of graphitization or the ratio of isotropic and anisotropic carbon forms, was not evaluated for this study, a possible link could exist between the maceral composition and rank and the resulting level of graphitization of the anthracite chars. This will be investigate in due course.

Porosity was not part of this study. Although pore development in the anthracites is expected to be low, its influence should be studied either to incorporate it in to the kinetic modelling or prove its negligible effect on the reactivity of the anthracites.

Ash content or composition on its own could not account for the different reaction rates. However, studying the phase distribution and the resulting composition of these phases under equilibrium condition could also not explain the different reaction rates of the reductants. The phase distributions and resulting compositions should be further investigated to characterize the mineral transformation during the Boudouard reaction at different temperature regimes.

Differences in the Boudouard reaction rates are most probably due to a combination of the carbon forms, how they change at high temperatures, and slag chemistry. The coating on the reductant particle could retard the reaction rate or act as a catalyst, depending on its composition.

References

1. KAHN, J.A. Non-rutile feedstock for the production of titanium, *Journal of Metals*, vol. 36, no. 7, 1984, pp. 33–38.

2. PISTORIUS, P.C. and COETZEE, C. Physicochemical aspects of titanium slag production and solidification. *Metallurgical and Materials Transactions B*, vol. 34B, October 2003, pp. 581–588.

3. PISTORIUS, P.C. Ilmenite smelting: the basics. *Journal of The Southern African Institute of Mining and Metallurgy*, vol. 108, 2008, pp. 35–43.

4. ZIETSMAN, J.H. and PISTORIUS, P.C. Process mechanisms in ilmenite smelting. *Journal of The Southern African Institute of Mining and Metallurgy,* December 2004, pp. 229–235.

5. GRAU, A. and POGGI, D. Physico-chemical properties of molten titania slags, J.M. Toguri and G.C. Weatherly (eds.) *Annual Volume of the Metallurgical Society of Canada*, Institute of Mining & Metallurgy, Montreal, 1978, pp. 97–102.

6. ZANG, L., HUANG, J., FANG, Y., and WANG, Y. Gasification reactivity and kinetics of typical chinese anthracite char with steam and CO_2. *Energy and Fuels*, vol. 20, 2006, pp. 1201–1210.

7. GRIGORE, M., SAKUROVS, R., FRENCH, D., and SAHAJWALLA, V. Influence of mineral matter on coke reactivity with carbon dioxide, *ISIJ International*, vol. 46, no. 4, 2006, pp. 503–512.

8. RUGHUBIR, N. and BESSINGER, D. Furnace dust from Exxaro Sands KZN. *6th International Heavy Minerals Conference*, The Southern African Institute of Mining and Metallurgy, 2007. pp. 43–48. ◆